J Neurophysiol
87: 2823–2834, 2002; 10.1152/jn.00628.2001.

Selectivity for Echo Spectral Interference and Delay in the Auditory Cortex of the Big Brown Bat *Eptesicus fuscus*

MARK I. SANDERSON AND JAMES A. SIMMONS
Department of Neuroscience, Brown University, Providence, Rhode Island 02912

Received 24 July 2001; accepted in final form 22 January 2002

Sanderson, Mark I. and James A. Simmons. Selectivity for echo spectral interference and delay in the auditory cortex of the big brown bat *Eptesicus fuscus*. *J Neurophysiol* 87: 2823–2834, 2002; 10.1152/jn.00628.2001. The acoustic environment for an echolocating bat can contain multiple objects that reflect echoes so closely separated in time that they are almost completely overlapping. This results in a single echo with a spectrum characterized by deep notches due to interference. The object of this study was to document the possible selectivity, or lack thereof, of auditory neurons to the temporal separation of biosonar signals on a coarse (ms) and fine (μs) temporal scale. We recorded single-unit activity from the auditory cortex of big brown bats while presenting four protocol designs using wideband FM signals. The protocols simulated a pair of partially overlapping echoes where the separation between the first and second echo varied between 0 and 72 μs, a pulse followed by a single echo at varying delay from 0 to 30 ms, a pulse followed at a fixed delay by a pair of partially overlapping echoes that had a varying temporal separation of 0–72 μs, and a pulse followed, with a varying delay between 0 and 30 ms, by a pair of echoes that themselves had a fixed temporal separation on a microsecond time scale. About half of the cortical units showed increased spike counts to pairs of partially overlapping echoes at particular separations (6–72 μs) compared with a baseline stimulus at 0-μs separation. For many neurons tested with a pulse followed by two overlapping echoes, we observed a sensitivity to the coarse delay between the pulse and pair of overlapping echoes and to the separation between the two echoes themselves. The sensitivity to the partial overlap between the two echoes was not tuned to a single temporal separation. For bats, this means that the absolute range to the closest reflector and range between reflectors may be jointly encoded across a small population of single units. There are several possible neuronal mechanisms for encoding the separation between two nearby echoes based on the sensitivity to spectral notches.

INTRODUCTION

For an echolocating bat to perceive distance, it must determine the time of occurrence for each echo relative to its vocalization or its "pulse" (Simmons 1971). This requires a separate volley of spikes for the pulse and for *each echo* at some point in the auditory system. Subsequent neurons in the midbrain, thalamus, and cortex selectively respond to the delay between pulse and echo and are thought to underlie the perception of target range (Feng et al. 1978; Olsen and Suga 1990; O'Neill and Suga 1982). Both the integration time of the cochlea (300–400 μs) (Simmons et al. 1989) and the absolute neural recovery time (500 μs) (Grinnell 1963) are sufficiently long to create a special problem for bats operating in typical sonar environments. Two echoes that are separated by less than ~300–500 μs will not be represented by separate spikes in a one-to-one temporal fashion in the brain stem (Casseday and Covey 1995). How do bats extract separate range information for the second echo when it is so close in time to the first?

Echoes that overlap with a separation of <300 μs interfere with each other, resulting in a single sound having spectral peaks and notches. A particular temporal separation gives rise to a specific spectral interference pattern or spectral shape. Behavioral studies support the idea that bats use spectral notch information to detect the presence of and compute the ranges between multiple closely spaced reflectors (e.g., Habersetzer and Volger 1983; Mogdans et al. 1993; Schmidt 1992; Simmons et al. 1974, 1990, 1998). Of particular interest are studies showing that bats actually perceive the ranges to the individual targets themselves not just a spectral coloration due to the overlapping echoes (for a discussion, see Simmons et al. 1990). Several computational studies discuss how the bat auditory system might estimate target structure, or the range of closely spaced reflecting points, using spectral information (Beuter 1980; Johnson 1980; Matsuo et al. 2001; Peremans and Hallam 1998; Saillant et al. 1993). However, few neurophysiological studies have explored the same issues using overlapping FM stimuli separated by <300–500 μs (Dear and Hart 1999).

The current study follows up previous work in the inferior colliculus (IC) of *Eptesicus fuscus* (Sanderson and Simmons 2000). The main finding was that neurons showed decreased activity if their best frequencies fell near the notch frequencies of overlapping FM signals. As suggested, but untested, by an earlier study, cortical neurons may select for particular temporal separations of overlapping echoes (Dear et al. 1993a). We were interested in seeing how cortical neurons responded to overlapping echoes, especially if they were more selective to interference notches than what was observed in the IC. In addition, we thought it was crucial that these studies be connected with our understanding of how the bat auditory system represents target range. Echoes at different delays return from objects at particular distances from the bat, and delay-tuned neurons should be tested for their selectivity to spectral properties of the echoes too. A classic delay-tuned neuron exhibits a facilitated response to a pair of sounds with a particular temporal interval; but are these neurons selective for both pulse-echo delay and the echo spectral profile simultaneously?

Address reprint requests to M. I. Sanderson (E-mail: Mark_Sanderson@Brown.edu).

The costs of publication of this article were defrayed in part by the payment of page charges. The article must therefore be hereby marked "*advertisement*" in accordance with 18 U.S.C. Section 1734 solely to indicate this fact.

If so, then single neurons can bind together two important target features—overall range to the target and the ranges between the component reflectors of the target itself.

Part of this work was presented at the annual meeting of Society for Neuroscience 2000.

METHODS

Surgical procedures

Animals were big brown bats (*E. fuscus*) obtained from houses in Rhode Island. The surgical procedures have been described before in Sanderson and Simmons (2000). Under isofluorane inhalation anesthesia, the skin and temporal muscles overlying the skull were cut and removed, and a specially prepared post was attached to the bone at the midline using cyanoacrylate gel. Following surgery, bats were allowed to recover for a minimum of 5 days before physiological recordings began.

On each recording day, the bat was placed in a plexiglas holder matched to its size and padded internally with sterile cotton. Thus restrained, the bat was suspended by a rubber band in a sound-proof booth (IAC), and the skull post was affixed in a rod secured by a setscrew. This set up immobilized the head and allowed for limited movement of the bat in the restraint. Craniotomies were performed each day using an operating microscope (Jena, Type 212) and a sharpened autoclaved sewing needle. The diameter of each craniotomy was between 50 and 150 μm. A tungsten microelectrode (FHC) was lowered slowly through the opening, viewed through the operating microscope, and was used to penetrate the dura. This tungsten electrode was subsequently removed and replaced with a hand-made carbon fiber electrode ($\sim$20 μm exposed tip length, 10-μm diam) (Fu and Lorden 1996), which was then lowered orthogonally to the cortical surface. Up to 25 craniotomies were made in each auditory cortex, and the position of each one was drawn on a map relative to the cortical vasculature visible through the skull. An indifferent tungsten electrode was inserted into the contralateral frontal cortex. We made our recordings in the same region as reported in Dear et al. (1993a) except that the overwhelming majority (141/144; 98%) of our craniotomies were made dorsal to the middle cerebral artery. We did not observe an obvious organization or clustering of any response properties other than best frequency, similar to the studies of Dear et al. (1993a) and Jen et al. (1989).

After the completion of the experiments, the bats were killed with an overdose of pentobarbitol sodium. The surgical and other experimental procedures were approved by the Brown University Institutional Animal Care and Use Committee and conformed to National Institutes of Health guidelines.

Stimulus generation

We created all stimuli using digital means. We developed a stimulus generation program using LABVIEW (National Instruments) running in a Pentium II computer to create FM sweeps. The program allowed for modifications of many signal parameters ($\leq$20 dB of attenuation, start and stop frequencies, duration, starting phase, number of harmonics, FM sweep shape, rise/fall duration, echo delay). The signals were created on-line and stored in memory as two data blocks corresponding to the two D/A channels available. On each trial, a pseudorandomly selected signal from each block was loaded onto one or the other D/A channel of a National Instruments PCI-6111e board.

An on-board counter triggered the D/A conversion process (500-kHz clock rate) for different repetition rates (typically 5 or 10 Hz) that were reasonable for driving cortical neurons in FM bats (Dear et al. 1993a; Tanaka et al. 1992). We repeated each stimulus usually for 16 or 32 trials. The analog signals from the two D/A channels were individually low-pass filtered (200 kHz, Wavtek model 442), additionally attenuated by $\leq$110 dB (Hewlett Packard 350 D), mixed together, and amplified (Apex PA02M high-voltage operation amplifier), before being sent to an ultrasonic loudspeaker (Panasonic leaftweeter, FAS-10TH1000). The speaker was located 38 cm from the bat, at 0° azimuth, 0° elevation relative to the bat's eye-nostril coordinates in the sound proof booth. We measured the system response with a 1/4-in Bruel and Kjaer microphone placed at the position of the bat's ear. The frequency response was flat ($\pm$1 dB) from 20 to 70 kHz, with a gradual roll-off of 0.33 dB/kHz $>$70 kHz. Second harmonic distortion was $<$50 dB from 10 to 100 kHz.

Data collection

The physiological signal from the electrode was amplified (WPI dAMP 80, 10,000 times) and band-pass filtered (Rockland Model 442, 200–8,000 Hz) before being sent to the A/D board. Starting with the first stimulus trigger, a simultaneous A/D conversion process began running on the PCI-6111e board. This conversion ran continuously, sampling the physiological signal at a 20-kHz rate (12-bit resolution). At the end of the entire stimulus set (typically 0.5–2 min), the physiological record was written to disk and then loaded into a data analysis program (LABVIEW) for initial spike waveform thresholding.

The next step, in the MATLAB environment, employed a user-operated spike-clustering method based on seven waveform features (e.g., voltage at time t_1, peak height, latency to peak) to extract single-unit activity from the thresholded events. The user selected cluster boundaries from six scatterplots of the waveform feature values (e.g., voltage at time t_1 vs. peak-to-valley height). Single-unit data formed tight clusters in the scatterplots and rarely had any intervals $<$2 ms in inter-spike interval histograms. Spike waveform shape had to be consistent from the beginning to the end of the experiment to be classified as a single unit. Seventy-two percent (94/130) of the recording sites in this paper had only a single clear cluster in the scatterplots. The spike profiles from a site that had two clear clusters in the scatterplots are shown in Fig. 3.

Thus isolated, spike times were plotted as dot rasters, peristimulus time histograms, spike counts, or latency functions in a manner appropriate for each stimulus set. These graphical displays were available immediately to guide the choice of subsequent stimulus parameters during the experiment. We performed the final cluster-cutting of single units off-line using the same MATLAB clustering program described above. Each recording session lasted between 5 and 7 h. The bat was awake and frequently took water and small portions of crushed mealworms throughout the course of an experiment.

Stimuli

A schematic for the four FM stimulus protocols is shown in Fig. 2. In these protocols, the "root" FM stimulus was composed of two harmonics that swept hyperbolically from 100 $\rightarrow$ 40 and 50 $\rightarrow$ 20 kHz (Fig. 1*A*). Durations were typically 2, 10, or 20 ms, with a linear rise-fall time of 0.3-ms duration.

PROTOCOL 1. Partially overlapping FM signals (refer to Fig. 2*A*). The first protocol simulated the waveform reflected from an object that contained two points, such as the wing and body of an insect (Simmons and Chen 1989). Each reflector, or "glint," returns a duplicate of the incident sonar sound with a temporal separation depending on the distance between the reflectors. For simplicity, we set the glints at the same amplitude. We simulated this compound echo by adding together two of the "root" FM signals into the same digital waveform file. An example of adding two root waveforms and the resulting waveform is shown in Fig. 1*B* ($S + S_{\text{delayed}} \rightarrow$ 34-μs separation). This two-part sound was delivered at 60 dB SPL *by itself*, without being preceded by a simulated broadcast sound. For some neurons, the stimuli were also presented at 80 dB SPL. Typical

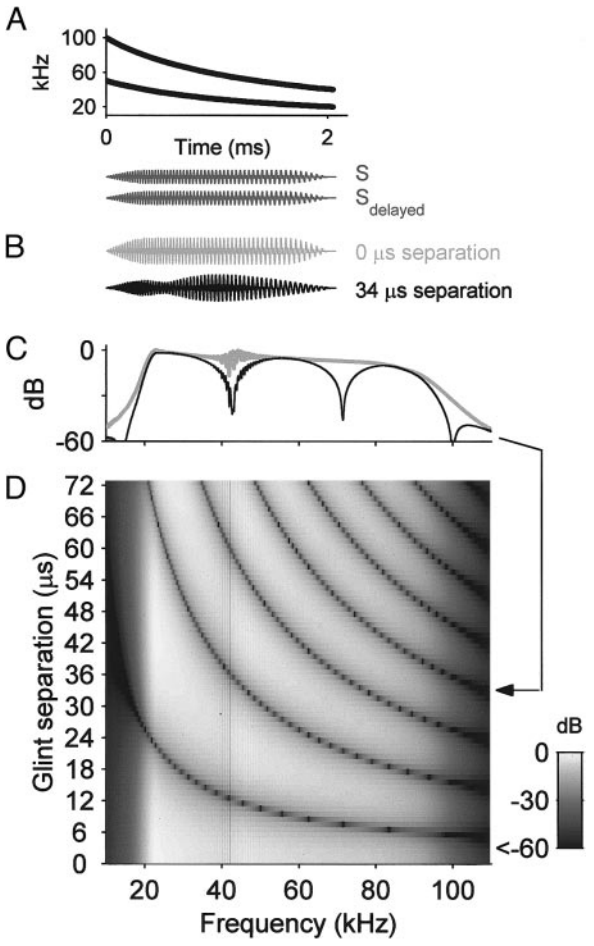

FIG. 1. Stimulus waveforms and spectra. *A*: the spectrogram for the "root" FM signal used in these experiments is shown at *top*. It consisted of 2 harmonics that hyperbolically swept from 50 to 20 kHz and 100–40 kHz. Typical durations were 2, 10, or 20 ms. *B*: to create overlapping FM stimuli we added the root FM signal (*S*) to a delayed copy ($S_{delayed}$). The resulting waveforms for 2 examples of paired FM signals separated by 0 and 34 μs. *C*: spectra for the 2 example waveforms. The spectrum for the FM pair with 0-μs separation is considered to be the "flat-spectrum" stimulus (gray). The spectrum for the FM pair with 34-μs separation has 2 prominent notches at ~44 and 74 kHz. *D*: surface plot of spectra for a typical stimulus set where separation between the 2 FM signals varied between 0 and 72 μs.

temporal separations between the first and second signal ranged between 0 and 72 μs in 3-μs steps (simulating 2 reflectors spaced 0–1.24 cm apart). We digitally created the signals by simply delaying and adding the root FM signal to itself (Fig. 1*B*). To accommodate temporal separations that required a noninteger separation in terms of samples (e.g., for a 3-μs separation at 500-kHz sample rate, the 2nd FM signal has to be delayed from the first by 1.5 samples), we originally created the signals at 1 MHz, performed the delay and add operation, and then downsampled to 500 kHz before loading them onto the D/A board. We refer to these paired FM stimuli as "2-glint" sounds throughout the paper (or as 2-glint echoes, when they are preceded by a simulated sonar broadcast in Protocol III).

The baseline stimulus was the completely overlapping condition, when the separation between the first and second root signal is 0 μs. Varying the time separation between the two FM signals added together creates a pattern of spectral notches that follows the hyperbolic relationship in *Eq. 1*

$$f_{notch}(n) = (2n + 1)/2\tau \qquad n = 0, 1, 2, 3, \ldots . \tag{1}$$

where τ is the separation in milliseconds between the first and second FM signal, f is frequency in kHz, and n is the notch number. To display all of the spectra for stimuli in protocol 1, we computed their Fast Fourier Transforms (FFTs), arranged the output in a matrix, and show the surface in Fig. 1*D*. The FFT for baseline stimulus (light gray in Fig. 1*C*) is found in the *bottom row* of the surface in Fig. 1*D*, and the position for FFT of the 34-μs, 2-glint signal is indicated by the arrow. Looking down on the surface three points are apparent: no stimulus has energy in a particular frequency bin that is greater than the baseline stimulus, the number of notches in the stimulus passband increases with increasing 2-glint separation, and the position of the notches follow the hyperbolic function of *Eq. 1*.

The baseline spectrum, for 0-μs separation, was considered to be a flat-spectrum stimulus because there are no prominent peaks or valleys in the spectrum from ~80 to 22 kHz (see the light gray FFT in Fig. 1*C*). We disregarded the high-frequency oscillation in the spectrum around 45 kHz that was due to applying an FFT on a two-harmonic signal. On a broad frequency scale, the spectrum in Fig. 1*C* actually slopes gently downward from 22 to 80 kHz; however, this is a gradual enough slope so that throughout the paper we will refer to this as the "flat" spectrum stimulus.

PROTOCOL 2. Pulse and echo at different delays (refer to Fig. 2*B*). The second stimulus protocol simulated *E. fuscus*' outgoing sonar emission and an echo from a single-point object at various distances from the bat. The root FM stimulus was presented at 80 dB SPL and was followed by the same FM stimulus but at 60 dB SPL at a delay between 0 and 30 ms. We chose these amplitude values based on the mean best pulse and echo amplitudes determined by Dear et al. (1993a) (78 and 57 dB SPL, respectively). In these experiments, a loud sound (80 dB SPL) followed by a soft sound (60 dB SPL) constitutes a pulse-echo pair. The presentation of the pulse alone and the echo alone was randomly interleaved among the presentations of the pulse-echo pairs for each trial. An important note is that the *echo alone* in protocol 2 is identical to the *baseline* stimulus from protocol 1 presented at 60 dB SPL.

PROTOCOL 3. Pulse and 2-glint echo (constant pulse-$echo_1$ delay; varied $echo_1$-$echo_2$ separation; refer to Fig. 2*C*). The third stimulus protocol simulated a pulse and echo from an object composed of two reflectors with variable spacing but at a fixed overall distance from the bat. In this protocol, a pulse at 80 dB SPL was paired with two echoes, each at 54 dB SPL. The delay between the pulse and the first echo was fixed at one value, Δt_1 (usually in the range 3–27 ms) The delay between the pulse and second echo, Δt_2, varied from Δt_1 to Δt_1 + 72 μs, in 3-μs steps. When the delay $\Delta t_2 = \Delta t_1$, (i.e., 0-μs separation) the resulting 2-glint echo was identical to the echo stimulus in protocol 2.

PROTOCOL 4. Pulse and 2-glint echo (varied pulse-$echo_1$ delay; constant $echo_1$-$echo_2$ separation; refer to Fig. 2*D*). The fourth protocol simulated an outgoing pulse and returning echo from an object composed of two reflectors; the object's two-point spacing remained fixed, but its overall distance from the bat varied. For this protocol, a pulse was paired with two echoes. The delay between the pulse and the first echo, Δt_1, usually varied from 0 to 30 ms. The delay between the pulse and second echo, Δt_2, was set to Δt_1 plus a constant value. The presentation of the pulse alone and the 2-glint echo alone was randomly interleaved among the presentations of the pulse-2–glint echo pairs for each trial.

When searching for neurons, we presented a series of FM sweeps that simulated the biosonar pursuit sequence of *E. fuscus* from search phase to terminal "buzz": both the duration of and the interval between FM sweeps covaried from long to short (Simmons 1989). Based on the response to the pursuit sequence stimuli, we often had an initial idea of the possible preferred duration and/or repetition rate to use for the FM sweeps in protocols 1–4. We presented the FM stimuli of protocols 1–4 using "short," "medium," or "long" durations (typically 2, 10, or 20 ms) and presented stimuli at different repetition rates, typically 5 or 10 Hz.

Data analysis

The majority of analyses in this report use the mean number of spikes per stimulus presentation trial counted in a 100-ms window from the time of stimulus onset. Generally, we observed that auditory cortex neurons respond with 1–2 spikes per stimulus presentation (Dear et al. 1993a). Two conditions had to be satisfied for the mean spike count to be considered a response: mean number of spikes per trial $\geq$0.3 and the distribution of spike counts on a trial-by-trial basis had to be significantly different from that of the spontaneous spike counts (Wilcoxon rank sum test, $\alpha = 0.05$).

DELAY SENSITIVITY TO PAIRED FM SIGNALS (FIG. 2, PROTOCOLS 2 AND 4). Pulse-echo facilitation was tested by comparing the response to pulse-echo pairs to the sum of the response to the pulse alone and echo alone. *Equation 2* shows the facilitation index calculated for each delay condition (Dear and Suga 1995)

$$\text{facilitation index} = (R_{PE} - R_P - R_E)/(R_{PE} + R_P + R_E) \quad (2)$$

where R_{PE} is the response evoked by the pulse-echo pair, R_P is the response to pulse presented alone, and R_E is the response to the echo presented alone. We considered a response with a facilitation index $\geq$0.2 to be facilitated. This criterion corresponds to a 50% increase in response strength for the paired stimuli as compared with the sum of the responses to the same stimuli presented in isolation.

Two measures of the delay-sensitivity spike count function, best delay and delay-tuning width, were calculated. The stimulus delay that evoked the strongest response was called best delay (BD) if two conditions were satisfied. First, the facilitation index for that response had to be $\geq$0.2. Second, the region around the peak response was estimated by finding the closest delay values on either side of the putative BD that elicited $<$50% of the peak response. All stimuli beyond these "borders" of the local maximum had to evoke a response $<$50% of the maximum response. We measured the width of the linearly interpolated spike count function between the two points at 50% of BD (Sullivan 1982).

For neurons tested with both protocols 2 and 4, we also computed the bootstrapped average ($N_{bootstrap} = 256$) BD and width of the delay spike count functions. In the bootstrap procedure, a single synthetic spike count function was constructed in the following manner. First we sampled, with replacement, the spike counts over the trials available for the neuron under study (typically, $N_{trials} = 20$) for each of the pulse-echo delay values. The mean of the 20 re-sampled spike counts at each delay value constituted a single synthetic spike count function. The delay value corresponding to the peak of a spline fit to this re-sampled spike count was stored as the *n*th bootstrap estimate for BD. The width of the spline fit between the two points at 50% of BD was stored as the *n*th bootstrap estimate for width. This procedure was repeated 256 times, and the average and SD for BD and width computed.

RESULTS

A total of 139 single units were recorded from the auditory cortex of five bats (left hemisphere only, 2 bats; right hemisphere only, 1 bat; bilaterally, 2 bats). Units were recorded at depths ranging from 231 to 976 μm (mean: 564 $\pm$ 162 μm). Each unit was tested with at least one of the four experimental protocols shown in Fig. 2. It was difficult to completely characterize each neuron's response to all four stimulus protocols. In the first place, rapid identification of appropriate duration and/or repetition rate parameters necessary to evoke strong activity was not always possible. Second, many neurons could not be held long enough to complete the four protocols.

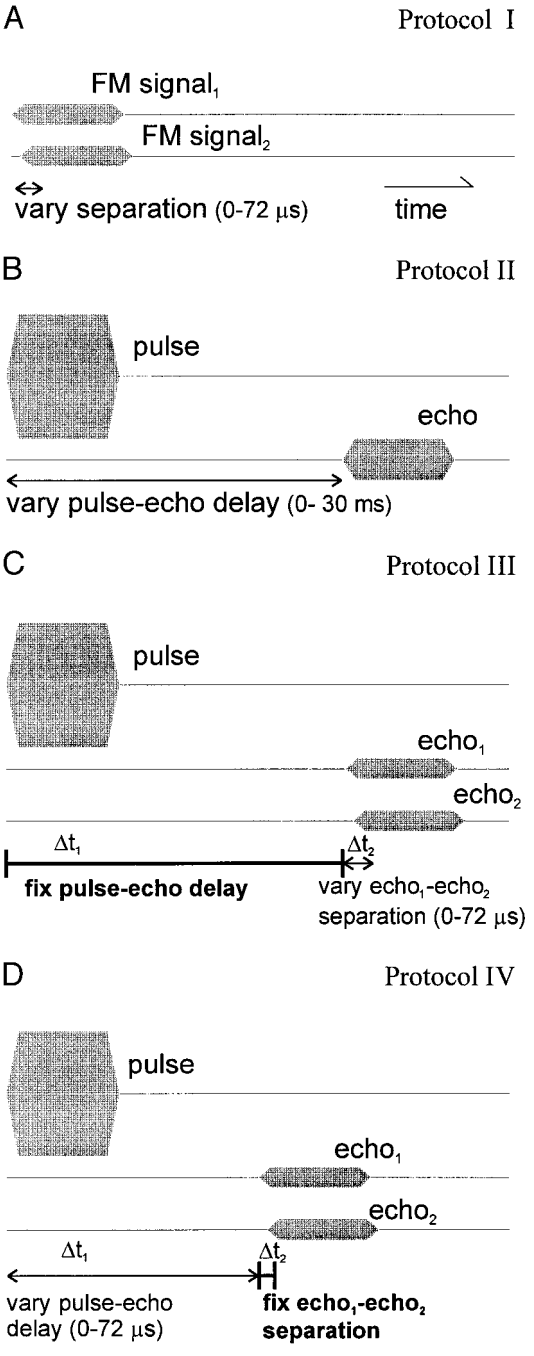

FIG. 2. Stimulus protocols. *A*: protocol 1 varied the temporal separation between 2 root FM signals shown in Fig. 1*A*. The amplitude of each was set so that when the separation was equal to 0 μs, the peak-to-peak amplitude of the resulting 2-glint signal was 60 dB SPL. *B*: protocol 2 varied the delay between 2 of the root FM signals over the range of 0–30 ms. The 1st signal of the pair had a fixed amplitude of 80 dB SPL and is called the "pulse." The 2nd FM signal was presented at 60 dB SPL and is called the "echo." The echo, in this case, was identical to the 2 FM signals of protocol 1 at 0-μs separation. *C*: protocol 3 consisted of a pulse followed by a 2-glint echo at a fixed delay. The 2-glint echo was identical to the stimuli in protocol 1. *D*: protocol 4 was a repeat of protocol 2 but used a 2-glint echo. In this case, the echo was composed of 2 FM signals with a non-0 temporal separation.

Protocol 1

PAIRED FM SIGNALS (0- TO 72-μS TIME SEPARATION). The first goal in our experiments was to characterize single-unit re-

sponses to paired wideband FM signals presented at 60 dB SPL. The separation between the two FM signals ranged from 0 to 72 μs and resulted in stimuli with flat (separation less than $\sim$5 μs) or notched (separation $>$5 μs) spectra (see Fig. 1*D*). Our primary interest was to detect a change, relative to a baseline, in a neuron's response to overlapping FM signals at different time separations. Baseline was always considered as the neuron's response to the "flat-spectrum" case—two FM signals with a separation of 0 μs. The median spike count for each stimulus condition was compared against the median spike count evoked by the baseline stimulus using the Wilcoxon rank sum test (2-tailed, $\alpha = 0.05$).

The responses to this stimulus set for two representative single units are plotted as dot rasters in Fig. 3, *A* and *B*. The mean number of spikes per trial for each stimulus condition is plotted for each neuron in Fig. 3, *C* and *D*, respectively. For the single unit in Fig. 3, *A* and *C*, activity decreased significantly for a particular subset of 2-glint separations relative to the baseline response (Fig. 3*C*, ○). No stimulus evoked activity statistically greater than the 2.25 spikes/trial for the baseline condition. The spike count function in Fig. 3*C* was similar to single-unit responses observed in the inferior colliculus: $\sim$1–2 spikes per trial for the 0-μs condition and one or more local minima for separations $\geq$6 μs (Sanderson and Simmons 2000). In contrast, the neuron in Fig. 3, *B* and *D*, did not even respond to the baseline condition (the response was not significantly different from spontaneous activity). However, this neuron did respond with a significant increase in activity to 2-glint separations of 27 and 60–63 μs.

Spike count functions of this type were generated for 84 single units in response to paired FM signals at 60 dB SPL. We divided the spike count functions into four categories based on the response to two FM signals with 0-μs separation. The first category included neurons that exhibited one or more local

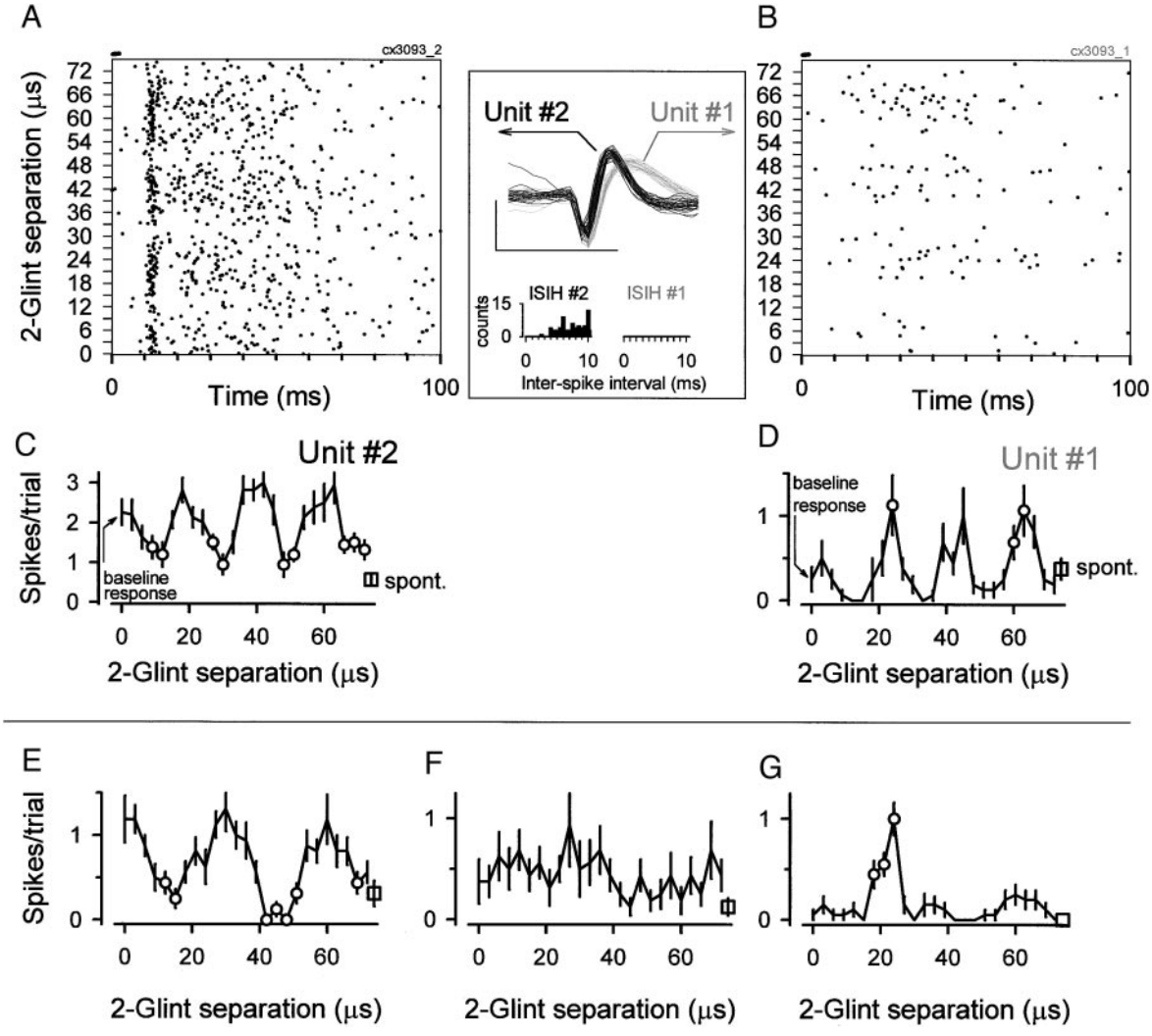

FIG. 3. Responses to 2-glint signals. *A*: dot rasters collected for different separations between a pair of FM signals (protocol 1). Each tick mark on the ordinate corresponds to 1st trial (of 16) for the corresponding 2-glint separation indicated at *left*. This single unit was recorded simultaneously on the same electrode with another, the dot raster for which is shown in *B*. The spike profiles and interspike interval histograms for the 2 units are shown *between A* and *B* (scale bars: 1 ms, 200 μV). *C*: the mean number of spikes per trial for the neuron in *A*. The vertical ticks around each mean spike count indicate standard error. ○, spike counts significantly different from the baseline condition, the 0-μs, 2-glint separation (Wilcoxon rank sum test, $P < 0.05$). The mean spontaneous activity counted in the same time window (0–100 ms), when no stimulus presented, is shown as a square at the *far right*. *D*: mean spike counts for data in *B*. *E–G*: additional examples from 3 single units. Stimulus duration and repetition rate: *C* and *D*, 2 ms, 10 Hz; *E*, 20 ms, 8 Hz; *F* and *G*, 10 ms, 10 Hz. Stimulus bar depicting duration and onset at *top* of *A* and *B*.

minima, *but no maxima*, in the spike count relative to paired FM signals with 0-μs separation (11/84, 13%; examples in Fig. 3, *C* and *E*). The second category included neurons that exhibited one or more local maxima in the spike count relative to paired FM signals with 0-μs separation (29/84, 35%; examples in Fig. 3, *D* and *G*). This category could also include neurons with responses that had local minima (8/29, 28%; e.g., see the spike count function for protocol 1 in Fig. 6*B*). The remaining responsive neurons did not show any clear pattern in their spike count function—no stimulus evoked a spike count that was statistically different from the baseline condition (16/84, 19%; example in Fig. 3*F*). The last category included neurons that were unresponsive to these stimuli at the repetition rates and durations tested—no stimulus evoked a spike count that was statistically different from spontaneous activity (28/84, 33%; example in Fig. 5*A*).

INTENSITY EFFECTS. We also presented protocol 1 at 80 dB SPL to a subset ($n = 57/84$, 68%) of the neurons and compared the results for the same neurons with 60 dB SPL data. Only 4 (7%) neurons exhibited similar responses at both amplitude levels (by "similar" we mean that the spike count functions for the 2 amplitudes had a positive, significant Spearman correlation coefficient, $P < 0.05$; e.g., Fig. 4*C*). In general, half of the neurons responded more strongly to one amplitude as compared with the other (based on median spike count over all stimuli, Wilcoxon signed-rank test, $P < 0.05$). For example, 23/57 (40%) neurons responded more strongly to the 2-glint FM stimuli at 80 versus 60 dB SPL (Fig. 4*A*). Alternatively, 10/57 (18%) neurons responded more strongly to stimuli presented at 60 dB SPL (Fig. 4*B*). The remaining neurons either were not strongly driven by paired FM stimuli (5/54, 9%) or displayed undifferentiated response functions at the two amplitudes (19/57, 33%).

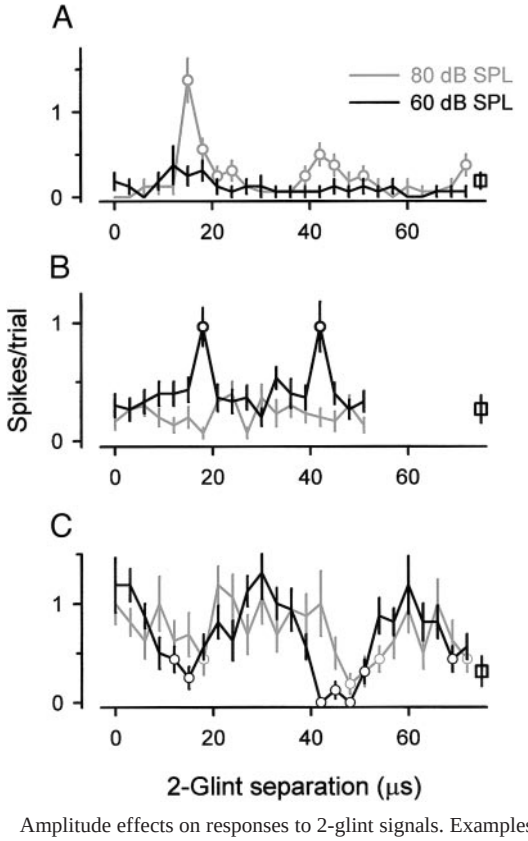

FIG. 4. Amplitude effects on responses to 2-glint signals. Examples from 3 neurons show effects of presenting protocol 1 at 2 different amplitudes (60 and 80 dB SPL). For most neurons, the spike count functions changed drastically with a 20-dB amplitude change. Duration and repetition rate for the 3 neurons: *A*, 20 ms, 10 Hz; *B*, 12 ms, 8 Hz; ,*C* 20 ms, 8 Hz.

Protocol 2: paired FM signals (0- to 30-ms separation)

The results thus far have concerned pairs of FM signals with rather short temporal separations (0–72 μs). These stimuli simulate a compound echo from an ideal two-point object. To simulate the sounds a bat may hear during echolocation, we also tested these neurons with a pulse-echo protocol. In these experiments an additional FM signal (pulse) preceded an identical, but attenuated, signal (echo; protocol 2, Fig. 2*B*).

We collected data from 117 neurons using a pulse-single echo protocol. Approximately half of the population (63/117, 54%) exhibited a facilitated response to pulse-echo pairs at some range of delays. The remaining neurons either responded to the stimuli but not in a facilitated manner (35/117, 30%) or did not respond at all (19/117, 16%). Forty-four of the delay-sensitive neurons (44/63, 70%) had a single peak in the facilitated pulse-echo delay response function, as defined in METHODS. The other various metrics measured from this data (BD, width at BD, correlation between width and BD, Q50%, and latency for the echo response at BD) were similar to those published previously by other groups (e.g., Dear et al. 1993a,b; Sullivan 1982).

Protocol 3: pulse and 2-glint echo at best delay

Using information from protocol 2, we next measured responses to FM signals as arranged in protocol 3 of Fig. 2*C*. In this protocol, we fixed the delay between a pulse and a 2-glint echo at BD (or the delay that evoked the strongest response in the data collected from protocol 2). This is simply a repeat of protocol 1 with the addition of a preceding pulse. We collected data for protocol 3 from 58 neurons.

To best illustrate protocol 3, we plot in Fig. 5 the results of running all four protocols on a single neuron. This neuron did not respond to FM pairs at 60 dB SPL with separations ranging from 0 to 72 μs (Fig. 5*A*). The response to the same stimuli at 80 dB SPL evoked no more than ~0.6 spikes per trial. When tested with the pulse-echo stimuli of protocol 2, the unit showed a facilitated response with a BD of 10 ms (Fig. 5*B*). We used these results to set the parameters for the next stimulus paradigm (protocol 3, Fig. 2*C*). Figure 5*C* shows the results when the 2-glint echo delay was fixed at 11 ms (Δt_1 in Fig. 2*C*) and separation between the two echoes varied from 0 to 72 μs (Δt_2 in Fig. 2*C*). With the addition of a preceding pulse at BD, the neuron exhibited a significant change in response to 2-glint echo separations as compared with the baseline 0-μs, 2-glint echo condition (Fig. 5*C*, ○). Using this result, we then retested delay sensitivity using a pulse paired with a 2-glint echo that had a separation of 9 μs (Fig. 5*D*). The actual experimental procedure for the collection of the data in Fig. 5*D* varied both delay (6–18 ms, Δt_1 in Fig. 2*D*) and echo two-glint separation (0 or 9 μs, Δt_2 in protocol 4, Fig. 2*D*) randomly for each stimulus presentation over the course of ~1.3 min. Under these conditions, the neuron responded more strongly to the two-glint echo with a 9-μs separation for every

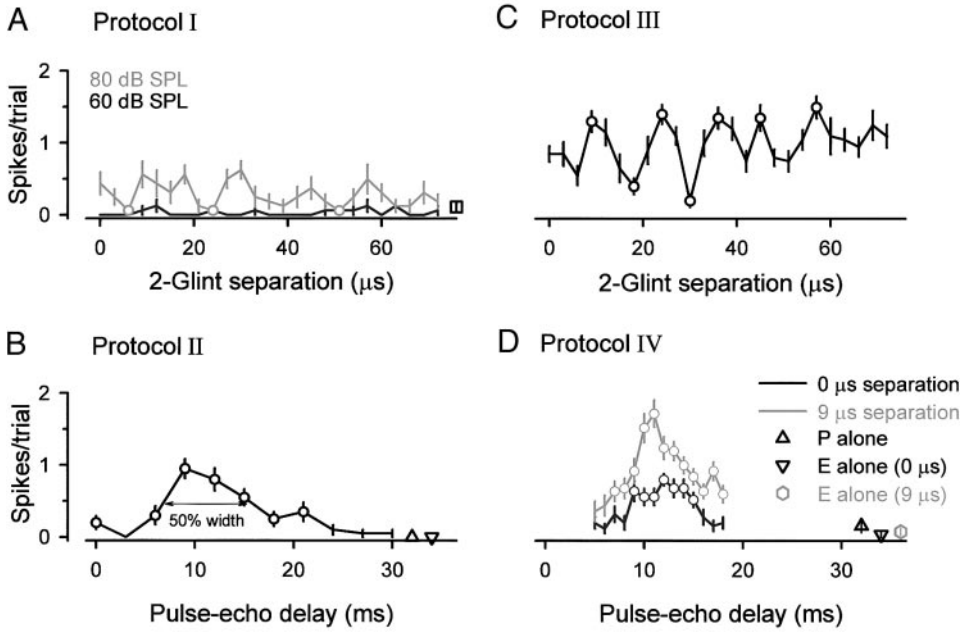

FIG. 5. Results from 4 stimulus protocols on a single unit. *A*: 2-glint stimuli of protocol 1 did not evoke a response for this neuron. *B*: the neuron responded with ~1 spike/trial for a pulse paired with an echo at 10-ms delay. ○, pulse-echo delays that resulted in a facilitated response. The response to the control stimuli, the pulse alone and echo alone, are plotted as △ and ▽, respectively. *C*: the repeat of the stimuli from *A* but paired with a preceding pulse offset by 11 ms. Now, particular 2-glint separations for the echo evoke activity that was significantly different from the 0-μs baseline condition (○). *D*: the basic pulse-echo delay protocol (2) was repeated, but this time the echo 2-glint separation was either 0 or 9 μs. All stimuli for these 4 protocols had a 2-ms duration and were presented at a 10-Hz repetition rate.

delay tested. The population results for protocol 4 are reported in the following text after those of protocol 3.

We grouped the responses from 58 neurons to protocol 3 into four categories based on the response to 2-glint echo with 0-μs separation. The first category included neurons that exhibited one or more local minima, but no maxima, in the spike count relative to the 2-glint echo with 0-μs separation (13/58, 22%). The second category included neurons that exhibited one or more local maxima in the spike count relative to the 2-glint echo with 0-μs separation (31/58, 53%; example in Fig. 6*A*). This category could also include neurons with responses that had local minima (14/31, 45%; e.g., see Fig. 5*C*). There were relatively few unresponsive neurons (4/58, 8%) because the parameters for this protocol were selected based on a significant response to previous stimulus protocols (see METHODS). The remaining neurons did not show any clear pattern in their spike count function (10/58, 17%).

A subset of these neurons was used in the following analysis (36/58).

Protocol 3 vs. 1: responses to 2-glint stimuli with and without a preceding pulse

We collected data from 36 neurons to compare the responses to 2-glint stimuli when presented in isolation versus being presented at a delay after a preceding pulse (protocol 1 vs. 3 in Fig. 2). We quantitatively summarized the results based simply on the difference of the median response strength across all stimuli between each condition (Wilcoxon rank sum test, significance assessed at $P < 0.005$). Figure 6 plots examples from the three possible categories that result from this analysis. The majority responded more strongly to the 2-glint stimulus when presented in tandem with a preceding pulse at BD ($n = 20$, example in Fig. 6*A*). Some neurons showed a greater overall response for the 2-glint stimuli presented without a preceding pulse ($n = 3$, example in Fig. 6*B*). The remaining neurons did not show any clear change in their overall response to the two conditions ($n = 13$, example in Fig. 6*C*).

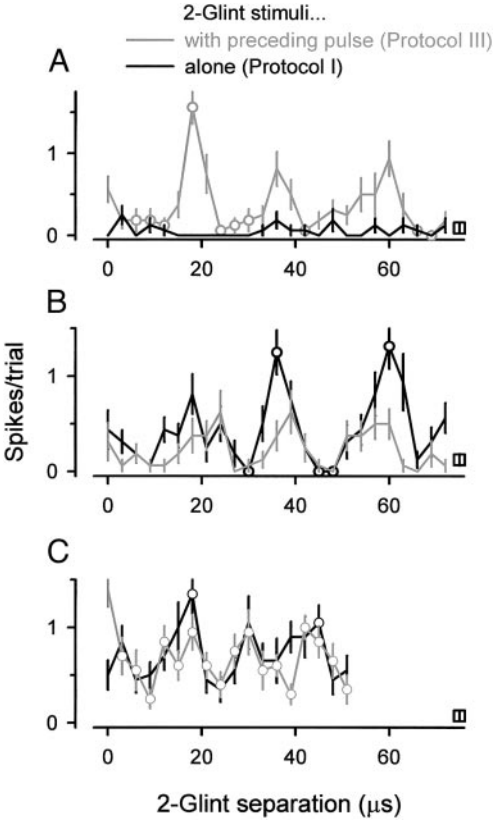

FIG. 6. Effect of preceding pulse on response to 2-glint signals. *A*: for some neurons, when the 2-glint stimuli was paired with a preceding pulse the response was increased relative the to 2-glint stimuli presented alone (this neuron did not even respond to the 2-glint stimuli presented without a pulse). *B*: some single units showed the opposite effect—an overall decrease in response when the 2-glint stimuli were paired with a preceding pulse. *C*: example of an unclear effect for the 2 stimulus conditions. Duration, repetition rate, and 2-glint echo delay value (τ_1 in Fig. 2*C*) for the 3 neurons: *A*, 2 ms, 5 Hz, 3 ms; *B*, 10 ms, 5 Hz, 7 ms; *C*, 5 ms, 10 Hz, 21 ms.

Protocol 4 vs. 2: 2-glint vs. "single" glint echoes

Most of the neurons tested with protocol 3 were also tested in protocol 4 (57/58). For these neurons, we examined how the delay sensitivity response functions changed for the echo 2-glint condition of a single versus double echo (protocol 2 vs. 4 in Fig. 2). Seventeen of these 57 neurons (30%) only showed a facilitated delay-sensitive response to a pulse paired with a 2-glint echo. These neurons either had no response (8/17, 47%) or an unfacilitated response (9/17, 53%) to the pulse paired with the flat-spectrum echo of protocol 2. These neurons were considered to be candidates for selectively signaling the presence of complex (i.e., "non-flat-spectrum" echoes) sonar targets. Our experimental method did not allow us to identify the relative proportion of these types of neurons because running protocol 4 required knowledge from protocols 1 or 3. Therefore our results tended to favor the case described next—neurons that showed a facilitated response to the stimuli of protocols 1 and 4.

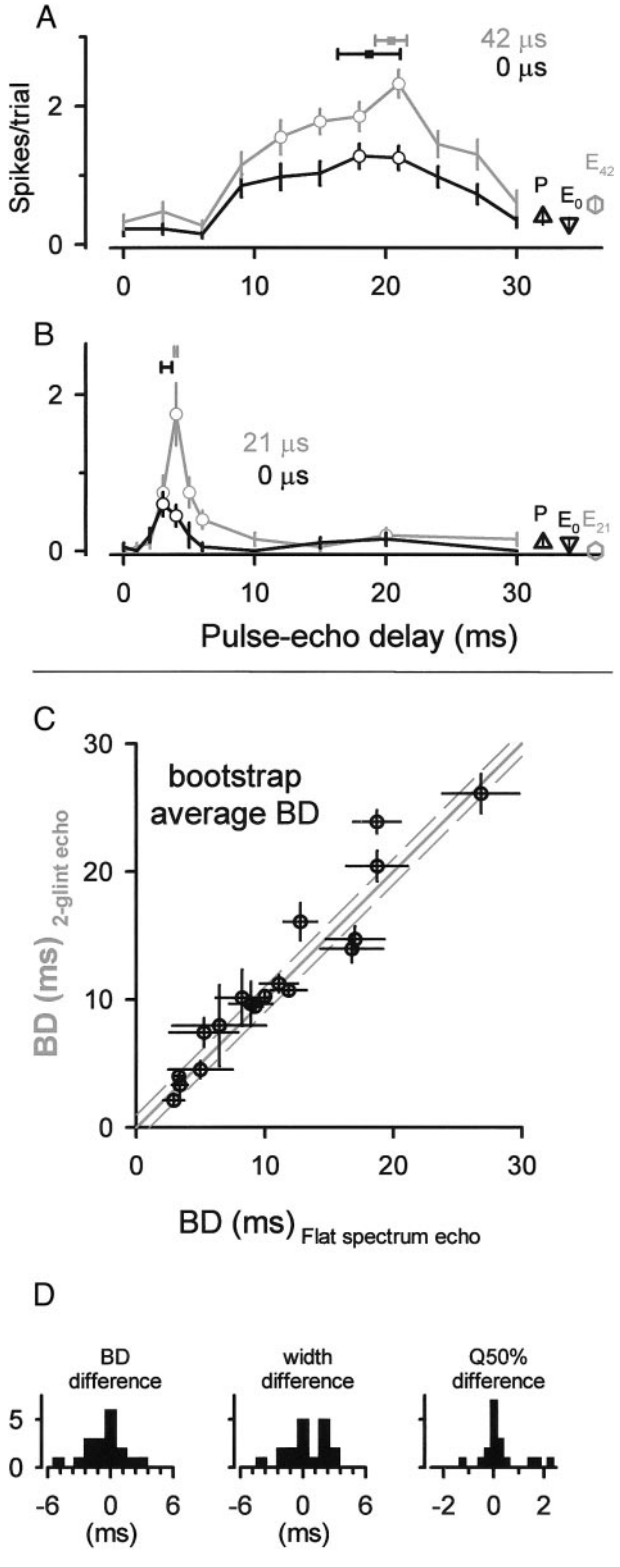

FIG. 7. Effect of echo 2-glint separation on best delay. *A* and *B*: responses from 2 neurons tested with different pulse-echo delays using 2 different echoes: a flat-spectrum echo (0-μs separation) and a notched-spectrum echo (where the 2-glint echo separation was set to a value determined from protocol 3, indicated by gray label). The bootstrapped average BD from based on 256 resamples of the raw spike counts is plotted as a small square above the mean spike count curves (squares are removed from the *bottom plot* for clarity). Horizontal bars are SD. Duration and repetition rate for the 2 neurons: *A*, 10 ms, 10 Hz; *B*, 10 ms, 5 Hz. *C*: bootstrap average BDs for the 2 echo conditions; 13/18 (72%) of the neurons had a BD shift <2 ms. Solid gray line is unity slope; dashed gray lines on either side are offset by 2 ms. *D*: distribution of differences for BD, width, and Q50% values. The value for the 2-glint condition was subtracted from the flat-spectrum condition.

Thirty-one neurons (31/57, 54%) exhibited facilitated responses to both a flat-spectrum single echo and an appropriately selected 2-glint echo. For each neuron, we expected the strongest response to the 2-glint echo condition would be greater than the strongest response to the flat-spectrum echo because we deliberately selected the 2-glint echo to be the best stimulus from protocol 3. The increase in the number of spikes for the pulse-2-glint echo stimulus was significant (median increase = 0.5 spikes, $P < 0.0001$, Wilcoxon signed-rank test, $n = 31$). Facilitation indices were also larger for the 2-glint echo condition (median increase = 0.0682, $P = 0.00295$, Wilcoxon signed-rank test, $n = 31$).

The literature on FM bats reports that the delay-sensitivity response function can change when any of a variety of pulse or echo stimulus features change. With changes in amplitude, duration, or repetition rate, the two typical neuronal response behaviors are that the amount of facilitation changes or BD shifts to a different value (Sullivan 1982; Tanaka et al. 1992). As noted in the preceding text, facilitation changed for most neurons when tested with particular 2-glint echoes in protocol 4. To test for BD shifts, we examined whether BD changed with changing 2-glint separation in those neurons that had an identifiable facilitated peak (18/31, 58%). We were cautious in assessing any change in BD simply from the peak of the spike count functions alone because we did not have a good measure of their variability. We could not simply measure the variability of BD *across trials* for two reasons: the total number of trials was rather small, usually ≤30 and the peak location could be undefined on a given trial because more than one pulse-echo delay could evoke identical and maximal spike counts (these neurons have a small dynamic range—0, 1, 2 spikes per stimulus). Therefore we used a bootstrap analysis to estimate the variability of the BD measure itself, and assess whether BD shifted when echo spectral properties changed (see METHODS).

Figure 7, *A* and *B*, shows the raw data from two neurons where pulse-echo delay responses were collected from proto-

cols 2 and 4. For each protocol, the bootstrap average BDs are plotted as square symbols with horizontal bars (±SD) at the top of each plot. For the most part, the presence of spectral notches had little effect on best delay. The estimated BD values from the two echo conditions were similar for most neurons (Fig. 7*C*), usually different by ≤2 ms (Fig. 7*D*). In addition, measures of the spike count functions' width did not change in a systematic fashion (Fig. 7*D*).

Protocols 3 and 4: sensitivity to target distance and spacing between target reflectors

We collected additional data for 21 neurons using protocol 4. This allowed us to loosely approximate the echo "receptive field" with respect to delay and echo 2-glint separation. The responses for three neurons are shown as three-dimensional plots in Fig. 8, *A–C*. For the most part, the results collected using the two different stimulus protocols are consistent. In Fig. 8*A* for example, when echo delay was varied and echo *2-glint separation* was fixed (black lines clustered closely together at 13, 15, or 17 μs), the results fall neatly beneath the results from the "orthogonal" experiment where *delay* was fixed and 2-glint separation varied (gray line). However, this did not hold in all cases as is evident in *B* when delay was varied for an echo with a 2-glint separation of 30 μs.

DISCUSSION

Behavioral studies on bats have shown that temporal and spectral information, specifically echo delay and echo spectral shape, are integrated to create the fundamental perceptual axis of target range (discussed by Simmons et al. 1990). How the auditory system extracts and eventually binds these two very differently represented acoustic features provides insight into the operations whereby a sensory system transforms information from the signal's dimensional space (time, frequency) into perceptual space (object size, texture, location).

Encoding the partial overlap between echoes (protocol 1)

One intriguing finding from this study was that 52% of the active neurons for protocol 1 responded weakly or not at all to flat-spectrum FM signals but showed an elevated response to FM signals with spectral notches (e.g., Fig. 3, *D* and *G*). Sanderson and Simmons (2000) observed a similar type of response in the IC to an identical protocol 1 stimulus set (except that the range of 2-glint separations for the IC study only spanned 0–24 μs instead of 0–72 μs as was used here). When analyzed using the same statistical test (Wilcoxon rank sum) used in the current paper, 23% (17/74) of the IC neurons exhibited an elevated spike count to a notched-spectrum FM stimulus compared with the flat-spectrum stimulus.

What creates the elevated response to a signal with one or more spectral notches as compared with a similar one without? One possibility might be a neural sensitivity to the apparent AM of the echo envelope that occurs due to the spectral notches when two echoes partially overlap (Miller and Pederson 1980). Throughout the bat auditory system exist neurons sensitive to AM (Llano and Feng 1999). However, the AM in our stimuli only occur when the signals are displayed in a wideband manner, such as on an oscilloscope or in Fig. 1*B*. When processed through band-pass filters as by the cochlea, the repetitive modulations in the signal envelope disappear

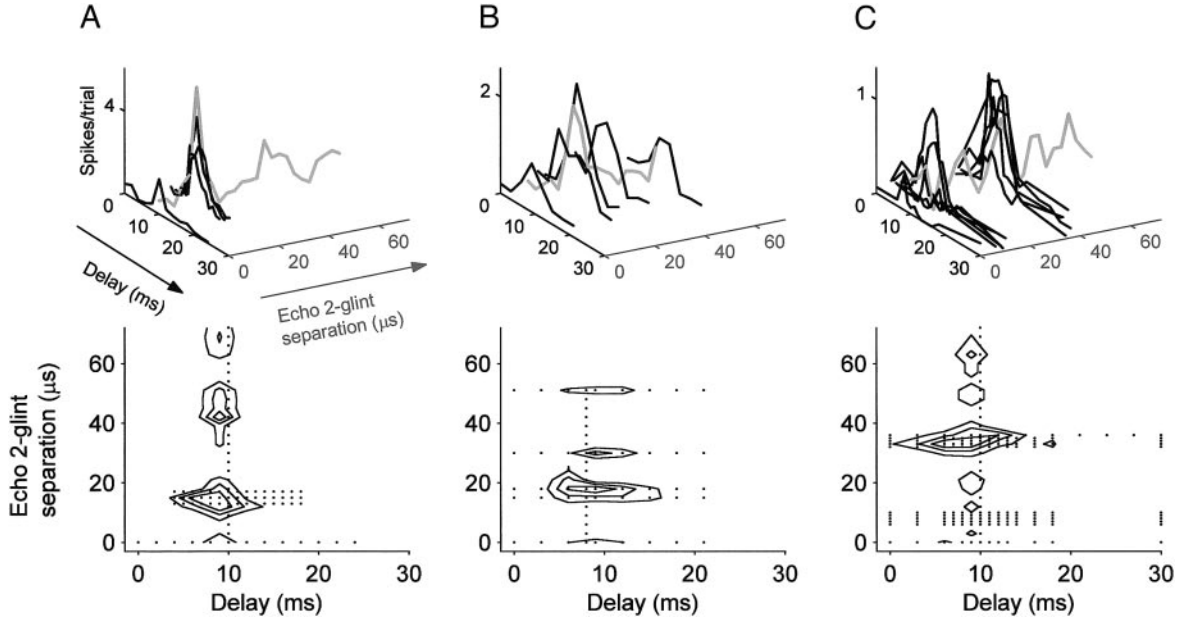

FIG. 8. Combination of spectral and temporal selectivity. *A*: single-unit response to stimuli with various pulse-echo delays (*x* axis) and echo 2-glint separations (*y* axis). Data from protocol 4 are plotted in black and aligned on the axis with the corresponding echo 2-glint separation (Δt_2 in Fig. 2*D*). Data from protocol 3 are plotted in gray and aligned with the *x* axis at delay value used in the experiment (10 ms, Δt_1 in Fig. 2*C*). This plot shows that data collected from the 2 different experimental protocols are fairly consistent. The contour plots of the same data are plotted below to facilitate comparison across the 3 neurons. Dots in the contour plot indicate the stimulus conditions presented. *B* and *C*: data for 2 additional neurons. The contour plot steps for neurons in *D–F* are 1.5, 0.65, and 0.62 spikes/trial. Duration and repetition rate for the 3 neurons: *A*, 10 ms, 10 Hz; *B*, 12 ms, 8 Hz; *C*, 2 ms, 10 Hz ms.

because they are produced by spectral notches at *different* frequencies occurring at *different* times.

A more likely explanation for the elevated responses observed in these neurons is a sensitivity to the spectral notch itself. This requires that a neuron has both excitatory and inhibitory frequency response areas, a common feature in *Eptesicus* cortical neurons (Jen and Chen 2000). A flat-spectrum echo will drive both the inhibitory and excitatory frequency regions, resulting in weak or no activity. In contrast, an appropriate notched-spectrum echo (with a spectral notch aligned over the inhibitory response area and energy in the excitatory frequency response area) can disinhibit the neuron, causing it to spike.

Measures of forward masking, nonmonotonicity, and tuning to ripple stimuli imply that inhibition is stronger in cortex as compared with subcortical regions (Barone et al. 1996; Brosche and Schreiner 1997; Depireux et al. 1996). This may lead to our observed difference in the relative proportion of neurons that show elevated responses to notched-spectrum stimuli in auditory cortex (52%) versus IC (23%). An increase in effective inhibition strength in auditory cortex could make neurons there reject wideband flat-spectrum sounds and selective for sounds with particular spectral notch patterns. Further evidence supporting this possibility is that every IC neuron responded to the flat-spectrum stimulus, whereas only 70% of the cortical neurons did (39/56; 3 examples of the 16 that *failed* to respond to the flat-spectrum stimulus are shown in Figs. 3, *D* and *G*, and 4*B*).

Representing specific spectral shapes requires neurons with complex spectral tuning curves that might be expected to consist of one or more inhibitory regions combined with one or more excitatory regions (cat cortex: Sutter et al. 1999; mustached bat midbrain: Portfors and Wenstrup 2000; mustached bat cortex: Kanwal et al. 1999). In this case, single neurons can represent local or nonlocal spectral shapes (Shamma et al. 1993). Further studies that carefully map the full frequency response area for *Eptesicus* cortical and collicular neurons are necessary. It would be useful to see if there were any common relationships in the excitatory and inhibitory regions of the response fields that corresponded to the typical position and number of spectral notches (Fig. 1*D*) for partially overlapping echoes (Dear et al. 1993a). In addition, the temporal dynamics and relative strengths of excitatory and inhibitory influences are probably crucial to predicting responses to overlapping FM signals.

Amplitude effects

Previous work in the IC showed a clear effect of overall stimulus amplitude on the 2-glint FM response functions. For most collicular neurons, the local minima in the response function to 2-glint stimuli became narrower and eventually disappeared with increasing stimulus amplitudes (Sanderson and Simmons 2000). We only presented protocol 1 at two amplitudes; to examine more systematically how the neurons' 2-glint response functions depend on level, future experiments should employ a wider range of behaviorally relevant amplitudes (e.g., at 20–60 dB SPL) (Kick and Simmons 1984).

Coarse (pulse-echo$_1$) and fine (echo$_1$-echo$_2$) delay sensitivity (protocol 3/4)

If a delay-sensitive neuron simply integrated excitatory inputs from the same frequency band for the pulse and echo, we would expect that no 2-glint separation would drive the neuron more strongly than the flat-spectrum echo in protocol 3. However, for half of the delay-sensitive neurons, this is not the case (protocol 3 results, e.g., Figs. 5*C* and 6*A*). In these neurons, we hypothesize that the spectral tuning to the pulse and echo was not identical. Evidence from several studies indicates that delay-sensitive neurons show the strongest facilitation when the pulse and echo are spectrally dissimilar (midbrain: Dear and Suga 1995; Portfors and Wenstrup 1999; thalamus: Olsen and Suga 1990; cortex: Berkowitz and Suga 1989; Paschal and Wong 1994). For mustached bats, this heteroharmonic tuning is related to the harmonic structure of the bat's echolocation emission and is thought to be useful for jamming avoidance. The heteroharmonic tuning in FM bats appears to be quite different and its functional significance is not well understood.

In the FM bat *Myotis lucifugus*, Paschal and Wong (1994) showed that the strongest responses from delay-sensitive cortical neurons came from pairs of mismatched (in terms of starting and stopping frequency) band-limited FM sweeps. We found that if the echo has a different spectral profile than the pulse (a more general kind of frequency mismatch), many neurons will show increased facilitation and response strength (Figs. 5*D* and 7, *A* and *B*). In some cases, neurons only exhibited delay sensitivity if the echo was different, spectrally, from the pulse.

Paschal and Wong's (1994) findings using mismatched pulse-echo FM pairs indicated that *all* of the neurons in bat auditory cortex are delay sensitive, provided that the pulse and echo have the correct spectral properties. Recent data from cat auditory cortex support a similar theme: neurons selective for temporal structure are also selective for spectral structure (Brosch and Schreiner 2000). Many cat primary auditory cortex neurons are most strongly facilitated by a particular pure tone interval with a one-octave frequency spacing between the two tones. They state that their work "raises the possibility that *all* neurons in auditory cortex are sequence selective when stimulated with the appropriate sequence" (Brosch and Schreiner 2000). For echolocating bats, the implication is that pulse-echo delay and echo spectral shape constitute the primary stimulus features extracted by the cortex.

The results from protocols 3 and 4, where a pulse precedes a pair of overlapping echoes, combines two relevant scales of the biosonar ranging axis. To be of any use to the bat, the separation between the two reflectors must be tied somehow to an estimate of the absolute range to the reflectors themselves. Figure 8 shows how this may happen in a select group of neurons: the three neurons are all tuned to ~10-ms delay but exhibit different selectivity to echo 2-glint separation. Together, these single neurons can represent the delay to the leading edge of two reflectors, in this case an object at 1.72 m. However, to decode the spacing *between* reflectors requires knowledge of the relative responses across a population because these neurons are not tuned to a restricted range of 2-glint separations.

Multiple echoes and spectral information in biosonar

The position and number of spectral notches are the most salient aspects of spectral shape as it applies to a biosonar signal when compared against the outgoing emission. For bats, an echo's spectral notches convey information about target position in one of two possible ways. First, as alluded to in the design of our experiments, the notches may result from the interference caused by two closely spaced reflectors. The number and position of notches is a function of the relative distance between the reflectors. Second, the multipath reflections from the pinna and tragus impose a spectral notch on echoes returning targets positioned below the horizontal (Wotton et al. 1995). These two spatial object properties, fine range and elevation, might confuse bats because a single spectral notch can arise due to an object's elevation or surface texture (Matsuo et al. 2001; Wotton et al. 1996). However, the bat's ability to intercept insects having different shapes shows that they can disambiguate shape from elevation (Griffin et al. 1965). Several versions of the same computational model (SCAT) (Saillant et al. 1993) have been developed to account for range and texture perception in bat sonar (Matsuo et al. 2001; Peremans and Hallam 1998; Saillant et al. 1993).

Mapping echo spectral shape information onto spatial axes is not straightforward due to several complexities. The spectral notch curves shown in Fig. 1*D* only hold for a situation where an object has two reflectors, each of which returns an echo with identical phase and amplitude. Altering the relative phase changes the position of the notches (translation on the frequency axis) and altering the amplitude affects the notch depth (Schmidt 1992). Worse yet, additional glints impose additional notches in the spectrum as a result of the combinatorial interference for each echo. Future work exploring how temporal delay and spectral shape information are represented in FM bats can provide valuable information about both general cross-correlation issues in the auditory system and how acoustic features are transformed into perceptual features.

We thank E. Bienenstock, S. Dear, and J. Fritz for advice and suggestions. J. Wotton, M. Ferragamo, and two anonymous reviewers provided very helpful comments on an earlier draft of the manuscript.

This work was supported by grants from the National Science Foundation (BES-9622297) and the Office of Naval Research (N00014-99-l-0350) to J. A. Simmons, a National Institutes of Health training grant, and a Burroughs-Wellcome pre-doctoral fellowship to M. I. Sanderson.

REFERENCES

BARONE P, CLAREY JC, IRONS WA, AND IMIG TJ. Cortical synthesis of azimuth-sensitive single-unit responses with nonmonotonic level tuning: a thalamocortical comparison in the cat. *J Neurophysiol* 75: 1206–1220, 1996.

BERKOWITZ A AND SUGA N. Neural mechanisms of ranging are different in two species of bats. *Hear Res* 41: 255–264, 1989.

BEUTER KJ. A new concept of echo evaluation in the auditory system of bats. In: *Animal Sonar Systems*, edited by Busnel R-G and Fish JF. New York: Plenum, 1980, p. 747–761.

BROSCH M AND SCHREINER CE. Time course of forward masking tuning curves in cat primary auditory cortex. *J Neurophysiol* 77: 923–943, 1997.

BROSCH M AND SCHREINER CE. Sequence sensitivity of neurons in cat primary auditory cortex. *Cereb Cortex* 10: 1115–1167, 2000.

CASSEDAY JH AND COVEY E. Mechanisms for analysis of auditory temporal patterns in the brain stem of echolocating bats. In: *Neural Representation of Temporal Patterns*, edited by Covey E, Hawkins H, and Port R. New York: Plenum, 1995, p. 25–51.

DEAR SP, FRITZ J, HARESIGN T, FERRAGAMO MJ, AND SIMMONS JA. Tonotopic and functional organization in the auditory cortex of the big brown bat *Eptesicus fuscus. J Neurophysiol* 70: 1988–2009, 1993a.

DEAR SP AND HART CB. Evidence for cortical potentials and the wavelet packet: a potential mechanisn for perceptual binding and conveying information. *Brain Lang* 66: 201–231, 1999.

DEAR SP, SIMMONS JA, AND FRITZ J. A possible neuronal basis for representation of acoustic scenes in auditory cortex of the big brown bat. *Nature* 364: 620–623, 1993b.

DEAR SP AND SUGA N. Delay-tuned neurons in the midbrain of the big brown bat. *J Neurophysiol* 73: 1084–1100, 1995.

DEPIREUX D, KOWALSKI NA, AND SHAMMA SA. Ripple analysis in the anterior auditory cortex and inferior colliculus of the ferret. *Assoc Res Otolaryn Abstr* 1996, p. 155.

FENG AS, SIMMONS JA, AND KICK SA. Echo detection and target ranging neurons in the auditory system of the bat *Eptesicus fuscus. Science* 202: 645–648, 1978.

FU J AND LORDEN JF. An easily constructed carbon fiber recording and microiontophoresis assembly. *J Neurosci Methods* 68: 247–251, 1996.

GRIFFIN DR, FRIEND JH, AND WEBSTER FA. Target discrimination by the echolocation of bats. *J Exp Zool* 158: 155–168, 1965.

GRINNELL AD. The neurophysiology of audition in bats: temporal parameters. *J Physiol (Lond)* 167: 67–96, 1963.

HABERSETZER J AND VOLGER B. Discrimination of surface-structured targets by the echolocating bat *Myotis myotis* during flight. *J Comp Physiol* 152: 275–282, 1983.

JEN PHS AND CHEN Q-C. GABAergic inhibition in frequency tuning of bat auditory cortical neurons. *Soc Neurosci Abstr* 26: 445, 2000.

JEN PH, SUN X, AND LIN PJ. Frequency and space representation in the primary auditory cortex of the frequency modulating bat *Eptesicus fuscus. J Comp Physiol [A]* 165: 1–14, 1989.

JOHNSON RA. Energy spectrum analysis in echolocation. In: *Animal Sonar Systems*, edited by Busnel R-G and Fish JF. New York: Plenum, 1980, p. 673–693.

KANWAL JS, FITZPATRICK DC, AND SUGA N. Facilitatory and inhibitory frequency tuning of combination-sensitive neurons in the primary auditory cortex of mustached bats. *J Neurophysiol* 82: 2327–2345, 1999.

KICK SA AND SIMMONS JA. Automatic gain control in the bat's sonar receiver and the neuroethology of echolocation. *J Neurosci* 4: 2705–2737, 1984.

LLANO DA AND FENG AS. Response characteristics of neurons in the medial geniculate body of the little brown bat to simple and temporally patterned sounds. *J Comp Physiol [A]* 184: 371–385, 1999.

MATSUO I, TANI J, AND YANO M. A model of echolocation of multiple targets in 3D space from a single emission. *J Acoust Soc Am* 110: 607–624, 2001.

MILLER LA AND PEDERSON SB. Echoes from insects processed using time-delayed spectroscopy. In: *Animal Sonar Systems*, edited by Busnel R-G and Fish JF. New York, Plenum, 1980, p. 803–807.

MOGDANS J, SCHNITZLER H-U, AND OSTWALD J. Discrimination of 2-wavefront echoes by the big brown bat *Eptesicus fuscus*: behavioral experiments and receiver simulations. *J Comp Physiol [A]* 172: 309–323, 1993.

OLSEN JF AND SUGA N. Combination-sensitive neurons in the medial geniculate body of the mustached bat: encoding target range information. *J Neurophysiol* 65: 1275–1296, 1990.

O'NEILL WE AND SUGA N. Encoding of target range and its representation in the auditory cortex of the mustached bat. *J Neurosci* 2: 17–31, 1982.

PASCHAL WG AND WONG D. Frequency organization of delay-sensitive neurons in the auditory cortex of the FM bat *Myotis lucifugus. J Neurophysiol* 72: 366–379, 1994.

PEREMANS H AND HALLAM J. The spectrogram correlation and transformation receiver revisited. *J Acoust Soc Am* 104: 1101–1110, 1998.

PORTFORS CV AND WENSTRUP JJ. Delay-tuned neurons in the inferior colliculus of the mustached bat: implications for analyses of target distance. *J Neurophysiol* 82: 1326–1338, 1999.

PORTFORS CV AND WENSTRUP JJ. Complex spectral responses in the inferior colliculus of the mustached bat. *Soc Neurosci Abstr* 26: 446, 2000.

SAILLANT PA, SIMMONS JA, DEAR SP, AND MCMULLEN TA. A computational model of echo processing and acoustic imaging in frequency-modulated echolocating bats: the spectrogram correlation and transformation receiver. *J Acoust Soc Am* 94: 2691–2712, 1993.

SANDERSON MI AND SIMMONS JA. Neural responses to overlapping FM sounds in the inferior colliculus of echolocating bats. *J Neurophysiol* 83: 1840–1855, 2000.

SCHMIDT S. Perception of structured phantom targets in the echolocating bat *Megaderma lyra. J Acoust Soc Am* 91: 2203–2223, 1992.

SHAMMA SA, FLESHMAN JW, WISER PR, AND VERSNEL H. Organization of response areas in ferret primary auditory cortex. *J Neurophysiol* 69: 367–383, 1993.

SIMMONS JA. Echolocation in bats: signal processing echoes for target range. *Science* 171: 925–928, 1971.

SIMMONS JA. A view of the world through a bat's ear: the formation of acoustic images in echolocation. *Cognition* 33: 155–199, 1989.

SIMMONS JA AND CHEN L. The acoustic basis for target discrimination by FM bats. *J Acoust Soc Am* 86: 1333–1350, 1989.

SIMMONS JA, FERRAGAMO MJ, AND MOSS CF. Echo-delay resolution in sonar images of the big brown bat *Eptesicus fuscus. Proc Natl Acad Sci USA* 95: 12647–12652, 1998.

SIMMONS JA, FREEDMAN EG, STEVENSON SB, CHEN L, AND WOHLGENANT TJ. Clutter interference and the integration time of echoes in the echolocating bat *Eptesicus fuscus. J Acoust Soc Am* 86: 1318–1332, 1989.

SIMMONS JA, LAVENDER WA, LAVENDER BA, DOROSHOW CA, KIEFER SW, LIVINGSTON R, SCALLET AC, AND CROWLEY DE. Target structure and echo spectral discrimination by echolocating bats. *Science* 186: 1130–1132, 1974.

SIMMONS JA, MOSS CF, AND FERRAGAMO M. Convergence of temporal and spectral information into acoustic images of complex sonar targets perceived by the echolocating bat *Eptesicus fuscus. J Comp Physiol [A]* 166: 449–470, 1990.

SULLIVAN WE. Possible neural mechanisms of target distance coding in auditory system of the echolocating bat *Myotis lucifugus. J Neurophysiol* 48: 1033–1047 1982.

SUTTER ML, SCHREINER CE, MCLEAN M, O'CONNOR KN, AND LOFTUS WC. Organization of inhibitory frequency recpetive fields in cat primary auditory cortex. *J Neurophysiol* 82: 2358–2371, 1999.

TANAKA H, WONG D, AND TANIGUCHI I. The influence of stimulus duration on the delay tuning of cortical neurons in the FM bat *Myotis lucifugus. J Comp Physiol [A]* 171: 29–40, 1992.

WOTTON JM, HARESIGN T, FERRAGAMO MJ, AND SIMMONS JA. Sound source elevation and external ear cues influence the discrimination of spectral notches by the big brown bat *Eptesicus fuscus. J Acoust Soc Am* 100: 1764–1776, 1996.

WOTTON JM, HARESIGN T, AND SIMMONS JA. Spatially dependent acoustic cues generated by the external ear of the big brown bat *Eptesicus fuscus. J Acoust Soc Am* 98: 1423–1445, 1995.